

What can we learn from observational stellar time series?

J. Perdang¹ and Th. Serre²

¹ Institute of Astronomy, Madingley Road, Cambridge CB3 0HA, UK and Institut d’Astrophysique, 5, Avenue de Cointe, B-4000 Liège, Belgium*

² Observatoire de Paris, 5, Place Jules Janssen, F-92195 Meudon Principal Cedex, France

Received 12 September 1997 / Accepted 9 March 1998

Abstract. A synthetic stellar time series simulating the observational radial velocity curve of a variable star is generated as follows. A 2D Lattice Gas (LG) model adapted to mimic the nonlinear nonradial behaviour of a vibrationally unstable plane-parallel stellar atmosphere representative for Long Period Variables is integrated over some 15 cycles. The model exhibits a complex spatio-temporal behaviour, showing simultaneously localised zones of expansion and contraction. The vertical component of the velocity field averaged over the atmosphere defines a noisy, cyclic time signal which is filtered with a Neural Network (NN) device. The analysis of the filtered signal by the method of Global Flow Reconstruction demonstrates that the latter is reproduced by a low dimensional (=4) dynamical system.

The experiment is thus indicative that the actual high-dimensional fluid dynamics describing the full 3D behaviour of a real star possesses an approximately autonomous low-dimensional directly observable radial subdynamics which alone is accessible with the conventional global observational procedures. Comments are made on the relation between this observable subdynamics and the observationally hidden full dynamics of the star.

Key words: chaos – methods: data analysis – stars: oscillations

1. Introduction

It has repeatedly been pointed out that while the fluid dynamic equations specialised to deal with strictly *radial stellar model pulsations* exhibit low dimensional chaos as behaviour of highest complexity, there is no guarantee that the same property continues to hold for the variability of *real stars*.

In fact, the *radial* pulsation experiments by Kovacs and Buchler (1988), based on detailed models of RV Tauri stars and Semi-Regulars, have indicated that the attractor dimension remains low (≤ 3). On a more abstract side, Normal Form Analysis of the radial equations makes it clear that the latter can indeed always be reduced to a low-dimensional differential system (of dimension probably not exceeding 5 or 6; Perdang

1994). Alternatively, as was stressed some time ago (Perdang 1990,1991), the 3D hydrodynamic equations which capture the full free motions of the stellar matter cannot be reducible, in general, to a low-dimensional differential system. For it is a well-known property that as the non-adiabatic effects are turned off, the number of potentially unstable modes becomes unbounded. Accordingly, the real *nonradial* motions of genuine stars may exhibit chaos of arbitrarily high dimension.

It may be argued that since the high dimensional stellar dynamics manifests itself through the occurrence of unstable *g*-modes, it is attached with the irregular convective motions. In the context of stellar variability, on the other hand, we are concerned with describing *organised global pulsations* (radial modes and non-radial *p*-modes in a linear approximation) rather than with the details of the turbulent motions of convection. Only a finite and small number of *p*-modes can become unstable; accordingly the nonlinear manifestation of the *p*-modes should remain low-dimensional as well. The fallacy of the latter inference is that in a nonlinear regime the *p*-modes are coupled with the *g*-modes. Therefore, strictly speaking the turbulent behaviour of the latter is inherited by the former.

We should observe that even in the idealised case of a coupling reducing to a ‘small perturbation’, which we may perhaps simulate by an additive noise component in the equations (stochastic process with properly selected characteristics), we are not entitled a priori just to ignore the interaction. The superposition of a noisy effect on a nonlinear dynamics can produce qualitatively new types of irregular behaviour if the system possesses two or more close enough attractors. The dynamics then undergoes random switches between these attractors, thereby exhibiting a highly irregular time behaviour (cf. the experiments of randomly perturbed 2D maps in Perdang 1991 designed to mimic the perturbative effect of turbulent convection; cf. also an experiment by Goupil et al 1988).

In genuine stellar hydrodynamics, on the other hand, the perturbation is neither small, nor is it simply additive. In general, the perturbation itself depends on the signal we wish to calculate.

These remarks are made clear by the following formalism. Suppose the full stellar fluid dynamics is described by a dynamical system Δ represented by an ODE in normal form,

$$\Delta : d/dt Z = W(Z), \quad (1.1)$$

* Permanent address

with Z and $W(Z)$ the ‘position’ and ‘velocity’ in the phase space of Δ , of (high) dimension $d = \dim \Delta$. Set $Z=(Y, U)$, where Y is the d_o -dimensional array of the ‘relevant’ physical variables we are actually interested in in the pulsation problem (nonlinear prolongations of the critical radial and p -modes, corrected by thermal effects), and U is the collection of the remaining ‘uninteresting’ variables (including the modified g -modes). The first subset of d_o equations of (1.1) can be written

$$d/dt Y = V(Y) + C(Y, U), \quad (1.2)$$

where the second term of the right-hand side describes the coupling between the Y and U variables. A similar system holds for the second subset of $d - d_o \gg d_o$ variables U .

Next make the assumption that the latter variables exhibit a highly complex behaviour (since they characterise turbulent motions). It then becomes meaningful to mimic their properties by stochastic processes (e.g. Wiener processes, Levy processes, etc); thereby Eq. (1.2) transforms into a stochastic differential equation

$$d/dt Y = V(Y) + \beta(t; Y), \quad (1.2a)$$

where the array $\beta(t; Y)$ represents the appropriate stochastic processes (in general depending on Y).

If the coupling is negligible, then the relevant Y variables are described by an a priori known closed subdynamics Δ_o , namely an ODE of low dimension d_o

$$\Delta_o : d/dt Y = V(Y). \quad (1.3)$$

In the general case, the effect of the complex turbulent motions is to introduce a stochastic ‘perturbation’ to the unperturbed closed subdynamics Δ_o . Let $Y_o(t)$ then represent the solution of the subdynamics Δ_o ; let $Y(t)$ represent the subarray of the corresponding solution of the full dynamics Δ . The solution of the stochastic perturbation of the subdynamics, (Eq. 1.2.a), $Y_p(t)$, which we may formally write

$$Y_p(t) = Y_o(t) + \eta(t), \quad (1.4)$$

will then remain close to $Y(t)$ (in a statistical sense to be specified), provided that the stochastic process has been properly chosen. But we have no guarantee that it will remain close to the ‘unperturbed’ solution, $Y_o(t)$ (cf. the experiments quoted). Accordingly, in general, we have no guarantee either that the low dimensional closed subdynamics Δ_o is meaningful for describing the observations.

The above formal properties suggest that in the typical case of stars showing convective zones, the underlying realistic stellar dynamics Δ is of an irreducible *high dimension* d . If $y(t)$ is any *generic* time series determined by the independent stellar variables $Z(t)$, $y(t) = F(Z(t))$, then the dynamics of the latter, the *signal dynamics* Δ_* , empirically recoverable from an analysis of $y(t)$, inherits the high dimensionality d of the full stellar dynamics Δ with which it is equivalent (Takens’s theorem).

Notwithstanding the conclusion of high-dimensionality of Δ , there has been a growing interest in *approximating* the dynamics inferred from observable time series by dynamical systems of *low dimensions* (of type 1.3). This has been done for

the purposes of gap filling and short time prediction, and it has been extended to simulate stellar time series $y(t)$ globally over long time intervals.¹ The latter approach has indeed supplied a low-dimensional dynamics reproducing the lightcurve of R Scuti (Buchler et al 1996).

Several interpretations may be adduced to account for this result.

(1) On the one hand, one may argue that in the case of the observed variable objects analysed so far the closed subdynamics Δ_o essentially determines the observational signal, the effects of turbulent motions ($\beta(t; Y)$ in Eq. 1.2.a) playing a negligible part; the attractor of the subdynamics, on which the unperturbed system evolves, remains well separated from any other attractor, so that the stochastic disturbances cannot push the phase point out of its initial basin of attraction. Although a genuine physical effect, the correction $\eta(t)$ to the unperturbed solution, $Y_o(t)$ (Eq. 1.4), remains small and can be viewed as additive ‘noise’; the latter is eventually wiped out from the observed signal $y(t)$ by standard filtering.

If this interpretation holds, then the dynamics capturing the main aspects of stellar variability is the physically reasonably well understood subdynamics Δ_o (Eq. 1.3); the latter is then equivalent to the signal dynamics Δ_* , and hence directly supplied by observation. We have model-free access to the mathematical structure of the simplest dynamical system Δ_o consistent with observation. The knowledge of the structure of Δ_o provides in turn quantitative information on the basic physics of the pulsation.

We should mention that in the context of this interpretation the low dimensionality of the signal dynamics hinges on the smallness of the turbulent contributions. Line-width measurements indicate however that the latter condition is characteristically violated in stars in which turbulent convection is taking place.

(2) We propose here an alternative interpretation of the success of low-dimensional reconstructions of observed signals, which does not hinge on the constraint of smallness of the turbulent effects. We suggest that the observed time series $y(t)$ *lacks* the property of *genericity*. The signal $y(t)$ is not a typical general function of the physical variables of the system we observe, but instead it is some special combination of these variables with dynamical properties of its own. The signal dynamics Δ_* is then not equivalent with the dynamics of the detailed stellar pulsations, Δ (Eq. 1.1); nor is it equivalent with the easily interpreted subdynamics Δ_o (Eq. 1.3). Instead, it corresponds to a concealed subdynamics of Δ .²

¹ In the method adopted by Serre (1992; cf. also Serre et al 1991) the velocity $V(Y)$ (Eq. 1.3) is locally approximated by a polynomial in Y , in a trial phase space of low dimension (following an approach due to Farmer and Sidorovich 1987, 1988; cf. also Casdagli 1989). A more global representation of $V(Y)$, again in polynomial form, is proposed in Serre et al (1996).

² The formal possibility of this point is illustrated by a mechanical example. A measuring device registers a time series representing the total mechanical energy E of a nondissipative mechanical system (described by the dynamics Δ). This signal is then just a constant,

Proposal (2) may appear as violating the methodology of scientific parsimony: We need to posit a seemingly ad hoc signal property—namely non-genericity—to account for the low dimensionality of the observed signal dynamics. On the other hand, under (1) the low dimension could be explained without an extra assumption on the mathematical nature of the signal. Moreover, the pattern of the observed curves seems to be reproducible by the dynamics of radial motions, which are numerically accessible with the standard radial hydrocodes.

The difficulty with the straightforward interpretation (1) is that the arguments reviewed above make the hypothesis of radiality of the observed pulsations theoretically unlikely.

We now show that the claim of non-genericity of the observed stellar time series is perfectly substantiated.

For the sake of definiteness, suppose that $y(t)$ is the observer's radial velocity curve. Essentially this signal is the integral over the visible star surface of the projection of the local velocity, $\mathbf{v}(t, \mathbf{r})$, onto the line of sight. But such a spatial averaging operation (a) erases the contributions due to any local small-scale irregular surface motions (local turbulence); likewise, (b) it wipes out any small-scale regular motions obeying various symmetries; and (c) it smoothes the remaining components of the large-scale motions. In addition, the signal is an integral over a time interval (the time required to register an observational datapoint), so that short time local fluctuations are lost as well.

Accordingly, the signal variable $y(t)$ quantifies what may be called a *pulsation macrostate*, which is the only information accessible to a variable star observer with standard observational equipment. Just as a same macrostate of statistical mechanics is realised by a variety of different experimentally inaccessible microstates, so is a same pulsation macrostate the result of different detailed observationally concealed hydrodynamic states (*pulsation microstates*), as described by the full stellar fluid dynamics, Δ . The observed signal function $y(t)$ is then not sensitive to each individual independent stellar variable (component of Z); i.e. it cannot be a generic function of the actual physical variables Z .

From a knowledge of the time sequence of macrostates alone we cannot have access to the dynamics of the microstates. But from the existence of a dynamics of the pulsation microstates, namely the dynamics Δ , we know that there must exist a dynamics of the pulsation macrostates, namely a signal dynamics, Δ_* , which we consider in the form

$$\Delta_* : d/dt Y_* = W_*(Y_*), \quad (1.5)$$

generated by the dynamical system $\Delta_* : d/dt E = 0$ (an exact subsystem of Δ). The oscillation energy is an instance of an 'atypical', 'nongeneric' signal function of the physical variables of the underlying dynamics Δ . Suppose next that a signal E' equal to the total energy E plus ϵ times the kinetic oscillation energy, is registered (ϵ arbitrary, but small). Formally such a signal E' is generic. However, in the presence of observational noise exceeding the level ϵ , the generic correction is unobservable; practically, the observed noisy signal remains effectively nongeneric.

the signal itself being a generic function of the new variables Y_* , $y(t) = G(Y_*(t))$. The signal dynamics Δ_* is an exact or an approximate subdynamics of the actual stellar dynamics Δ . In principle it can be recovered from the latter through some appropriate 'projection' operation, in the same way as the equations of fluid mechanics are approximately generated from the dynamics of an interacting N -particle system. A priori the dimension d_* of the dynamics Δ_* is then expected to be lower than the dimension d of the full stellar dynamics, Δ .

(3) Our discussion was concerned so far with ideal noise-free signals. In the real *noisy* time series the dimension of the underlying signal dynamics will be typically underestimated. In fact, let $y(t)$ represent the observed noise-polluted signal, and denote by $s(t)$ the underlying pure signal we are actually interested in. The noise component is assumed to be characterised by a single measure ν which, for the sake of argument is identified here with the maximum local noise level; any other statistical measure just alters the form of the following argument without affecting its nature. The pure signal $s(t)$ is thereby constrained by the requirement that it must lie in an area of the y - t plane sandwiched between the two curves $y(t) + \nu$, $y(t) - \nu$. To solve the problem of finding a synthetic signal, $s_s(t)$, which is a unique estimate of the pure signal $s(t)$, we stipulate that (a) $s_s(t)$ is the 'simplest' smooth function defining a curve through the allowed area; and (b) $s_s(t) = H(Y_{**})$ is a generic function of a d_{**} -array of variables Y_{**} obeying an *estimated signal dynamics*

$$\Delta_{**} : d/dt Y_{**} = W_{**}(Y_{**}). \quad (1.6)$$

This estimated signal dynamics differs from the true signal dynamics (1.5) in so far that our stipulations of parsimony operate an extra smoothing on the pulsation macrostates; and this smoothing is the stronger the higher the noise level ν is. We necessarily have the inequalities

$$d_{**} \leq d_* \leq d. \quad (1.7)$$

³ Provided that the noise level ν is not too low, we are then certain of the existence of an estimated signal dynamics Δ_{**} of *finite* and *low* dimension d_{**} such that the simplicity conditions (a) and (b) are fulfilled. We insist once again that the estimated signal dynamics Δ_{**} is merely a surrogate of the true signal dynamics Δ_* responsible for the actual pure signal $s(t)$. The dynamics Δ_{**} then does not contain the true physics of the stellar pulsations; but it is the 'best approximation' to the mathematical structure of the latter consistent with our assumption (a,b) of parsimony.

³ Simplicity of the synthetic signal $s(t)$ is defined relative to a given framework, in the present case autonomous ODEs, with the property that for each such system there exists a Reduced Normal Form (Eq. 1.6) of lowest dimension d_{**} . The principal measure of simplicity is thus the dimension d_{**} ; as a secondary measure of simplicity the lowest algebraic degree n_{**} of the polynomial representation of each component of $W_{**}(Y_{**})$ is chosen. This rule of parsimony is indeed applied in the flow reconstruction (Sect. 4). In the case of intrinsic stellar variability we have good reasons to assume a priori that the star's behaviour is described by a dynamical system which can be represented in the form (1.1); the above criterion of parsimony then seems satisfactory, even though it is by no means unique.

Genuine stellar observations being typically very noisy, we should not be surprised to find an estimated signal dynamics of low dimension d_{**} associated with *any* noise-corrupted stellar time series $y(t)$.

A final general comment on the rôle of noise in time series $y(t)$ on the construction of an underlying dynamics is in order. Although observationally accessible at a finite number T of discrete instants only, say at times $t = t_o, t_o + 1, t_o + 2, \dots, t_o + T - 1 = t_1$, the signal $y(t)$ is naturally assumed to be defined for a *continuous* time t , ranging over the (compact) interval $[t_o, t_1]$, and to be a *smooth* and *bounded* function of its argument t . Under these assumptions the series can be uniformly approximated over $[t_o, t_1]$, by elementary analytic functions (truncated Fourier series, multiple Fourier series of low order, etc). Given a high enough noise level ν , *any* noisy empirical time series $y(t)$, whatever its physical origin, can always be approximated via some autonomous differential system (1.6) of low order d_{**} .

Care must then be exercised in interpreting this estimated signal dynamics Δ_{**} : It may indeed be a *fictitious dynamics* failing to reflect the physical mechanisms at the origin of the signal.⁴ The procedure of searching for an approximation of a signal dynamics in the form (1.6) is meaningful only if there is substantive evidence that the signal is generated by a dynamical system of form (1.1) in the first place.

The information carried by a signal dynamics Δ_* (Eq. 1.5), and more importantly by an estimated signal dynamics Δ_{**} (Eq. 1.6), can be summarised as follows.

(1) In the absence of any theoretical information on the physical origin of the empirical (noisy) signal $y(t)$, it is safest to view the estimated signal dynamics as a *fictitious dynamics*. No convincing conclusion on the true physics at the origin of the signal can then be drawn. However, a fictitious dynamics may still serve the purpose of a predictor for the empirical signal $y(t)$

⁴ An extreme instance illustrates this point. Take a real time series $s(t)$ generated by a Wiener process over $T + l$ timesteps t . Suppose that the observationally available series $y(t)$ is obtained by a measuring device that takes an average of the true series $s(t)$ over l successive timesteps

$$y(t) = \frac{1}{l} \sum_{\tau=0}^{l-1} s(t + \tau), \quad t = 0, 1, \dots, T - 1.$$

A correlation between l successive measured values, $y(t), y(t + 1), \dots, y(t + l)$, is thereby generated, so that the recorded series $y(t)$ exhibits a smooth and systematic trend together with a superposed noisy residual. If we then select a noise level higher than the residual noise, but less than the fluctuations of the Wiener process, then the estimated signal dynamics Δ_{**} (Eq. 1.6) associated with the noisy time series $y(t)$ according to the procedure outlined above, will provide an approximate copy of the signal $y(t)$. But the deterministic dynamics can only describe the artificially created trend in this function. Moreover, since $y(t)$ and $y(t + \tau)$ are uncorrelated if $\tau > l$, it is clear that the dynamics must be chaotic, of Lyapunov horizon $\leq l$. The signal dynamics reconstructed in this way is then entirely fictional; it has no relation with the intrinsic stochasticity of the original signal $s(t)$. The dynamics just simulates the effects of the deterministic operations and transformations carried out in the measuring apparatus.

(extrapolation and interpolation over time intervals less than the Lyapunov horizon).

(2) If we know a priori that the signal is generated by a dynamical system (Eq. 1.1), then we are entitled to interpret the estimated signal dynamics Δ_{**} as an approximation to the true signal dynamics Δ_* , and therefore as an approximate closed subdynamics of the full dynamics Δ (Eq. 1.1) of this physical system. Inequalities (1.7) then provide a *lower bound* for the dimension d .

(3) If we have substantial knowledge that the signal is a generic function of the dynamical system from which it originates, then the true signal dynamics is equivalent with the *full dynamics*, and hence $d = d_*$. Again, for a noisy signal only the estimated signal dynamics, and hence d_{**} is accessible.

In the case of intrinsic stellar variability as theoretically described by the equations of fluid dynamics, heat transfer, reaction kinetics, etc, alternative (2) applies. The signal dynamics then does carry partial information on the physics of the pulsations. However the information on the complexities of the 3D hydrodynamic motions is thrown away as a result of the various averagings inherent in the definition of the time series $y(t)$. Alternative (3) holds if we have reasons to regard the pulsations as strictly radial. Under those conditions full information on the pulsation physics is available from the true signal dynamics.

The purpose of this Paper is to shed some light on alternative (2). To this end we have analysed a theoretically generated time series $y(t)$ whose underlying dynamics is known. The micropulsational behaviour of an unstable extended stellar model atmosphere is followed on a 2D Cellular Automaton (CA) model. The time series $y(t)$ considered is the scalar observable ‘radial velocity curve’, $v(t)$, obtained from the instantaneous local velocity field, $\mathbf{v}(t; \mathbf{r})$, directly available in the simulations.

This stellar signal $y(t)$ is found to exhibit a sequence of cycles whose amplitudes and cycle-lengths change in a broadly smooth way, with superimposed irregular and often large fluctuations. These fluctuations are mainly due to ‘numerical noise’ (unavoidable in our small-scale CA simulation). We regard therefore $y(t)$ as a noisy signal. The fluctuations are filtered out, and a smooth cyclic observable, denoted $s(t)$, survives. The notation $s(t)$ refers here to an *approximation* to the pure signal, rather than to the pure signal describing the pulsational macrostate behaviour itself. On the other hand, the velocity field, $\mathbf{v}(t; \mathbf{r})$, i.e. the pulsational behaviour of the microstates of the atmosphere, is found to trace out extremely convoluted space structures at any given time. At a fixed position in space, the components of $\mathbf{v}(t; \mathbf{r})$ exhibit a highly irregular fluctuating time-behaviour, of amplitude nearly an order of magnitude larger than the amplitude of the macrostate variable $s(t)$. The spatial zone which is in a state of expansion is typically made up of a collection of disconnected patches whose numbers and sizes change with time; a maximum in the signal $y(t)$ provides a single piece of ‘scalar’ information about these regions, essentially the property that the total area of the expanding patches goes through a maximum. Smoothness in the time pattern of the (approximation to the) pulsational macrostate variable $s(t)$ is a consequence of the various filtering operations of $y(t)$.

It is then out of the question that a reconstruction of the complex space structure of the true hydrodynamic velocity field, $\mathbf{v}(t; \mathbf{r})$, should be made available from the pulsation macrostate observable $s(t)$, from which all short-time structure and all space structure has been ironed out: Takens's theorem applies to a construction of a macropulsation dynamics from the series $s(t)$. It manifestly fails to apply to the reconstruction of the micropulsation dynamics Δ , since most of the microdynamic information has been lost in the process of construction of the series $s(t)$.

2. Time series from a CA pulsation model

A rudimentary plane-parallel vibrationally unstable 2D stellar atmosphere model approximately representative for Long Period Variables is simulated on a CA. The pulsational behaviour is initiated by a vertical disturbance of the hydrostatic equilibrium state (analogue of a radial perturbation of a real star). The perturbation is then followed in time. After a transient phase, the configuration is observed to settle into a statistically steady state exhibiting complex small-scale motions.

Represent the instantaneous velocity field of the atmosphere at time t in Cartesian coordinates

$$\mathbf{v}(t; \mathbf{r}) = (v_x(t; x, z), v_z(t; x, z)) \quad (2.1)$$

(x, z , horizontal and vertical directions respectively). Define a time series as an average vertical velocity

$$y(t) \equiv \langle v_z(t; x, z) \rangle, \quad t = 0, 1, \dots, T-1, \quad (2.2)$$

the averaging being carried out (a) over *space* (integral over the whole 2D model atmosphere) and (b) over *time* (integral over $< \frac{1}{20}$ of the mean cycle length); the series is recorded at T equidistant instants of time. This signal is regarded as the formal counterpart of the variable star observer's *radial velocity curve*, $v(t)$. Although distinct global measures of the hydrodynamic motions in the star, $v(t)$ and $y(t)$ do indeed share two common features: (a) Intrinsically both signals result from the *same micropulsation dynamics*; and (b) both signals are *non-generic*; they are (distinct) macropulsation variables associated with the pulsational microstates.

The computational framework in which the fluid dynamics has been investigated is the LG atmosphere model discussed in Perdang (1993). The atmosphere is simulated on a small lattice (61×61 cells) containing a small number (1700) of LG particles. Accordingly our numerical results exhibit an amount of statistical noise in the micropulsation states much larger than the realistic statistical hydrodynamic noise. The spatial averaging over the whole lattice, and the additional smoothing over time eliminate part of this noisy component. We then regard the residual noise in $y(t)$ as the analogue of the observational noise in real stellar measurements.⁵

⁵ The LG model was applied to the simulation of Bénard convection (Lejeune et al 1994). In spite of the smallness of the lattice size and the number of particles, the model duplicates the convection pattern of regular rolls at low temperature gradients, and the irregular turbulent

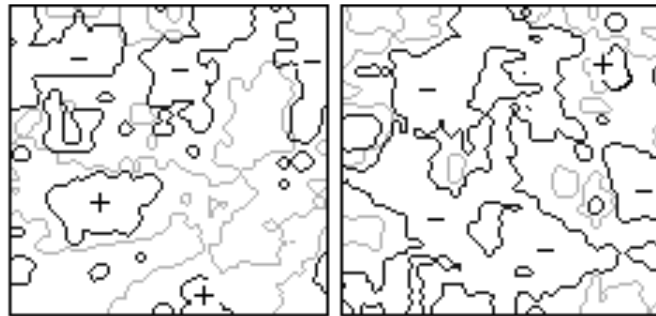


Fig. 1a and b. Two snapshots of the instantaneous vertical velocity contours; **a** left: close to global expansion; **b** right: close to global contraction; dark contours $v_z = +0.1$ (shown by +); grey contours $v_z = +0.05$ and dark contours $v_z = -0.05$ (-).

While CA fluctuations are necessarily exaggerated versions of the intrinsic hydrodynamic fluctuations, these fluctuations have the virtue of sharing at least one qualitative property of real hydrodynamic fluctuations: they can excite *any type of instability* that may manifest itself in the stellar medium. In the conventional hydrodynamic treatment instabilities may be missed because the formalism, in contrast to nature, does not automatically provide for excitations of them.

We have followed the perturbed LG atmosphere model over 4500 CA timesteps. To make sure that the transients have died out, and that we are well within the statistically stationary phase of small-scale motions, we consider the global time series $y(t)$ over the last 3000 computed timesteps. Fig. 1 provides an idea of the complexity of the pulsational microstates in the latter phase. It shows the instantaneous vertical velocity contours $v_z(t; x, z) = 0.1, 0.05$ and -0.05 (in CA units) near a maximum of the time series (average global expansion of the star), and near the subsequent minimum (global contraction); locally $|v_z(t; x, z)|$ exceeds the value 0.2.

Even though in our experiments the initial perturbation preserves the symmetry of the hydrostatic equilibrium, the original simple symmetry of the configuration is broken at later times (Fig. 1). In the transient phase the initially 'radial' velocity pattern suffers indeed a cascade of symmetry breakings. A permanent phase is then established, characterised by a statistically broadly stationary velocity pattern which however undergoes continual changes in its structural details. A qualitatively comparable but more violent scenario is well-known from direct 2D (and 3D) integrations of the initial phases of supernova explosions (Fryxell et al 1991; Hachisu et al 1990; Benz and Herant 1993). The similarity of both structural patterns gives us confidence that our qualitatively new results are not just numerical artifacts.

In the stage of the stationary atmosphere motions we isolate a clear-cut cyclic behaviour in the noisy macropulsation variable $y(t)$. A phase of global contraction, $y(t) < 0$, [expansion, convective motions at high gradients. The experiment gives us confidence that the low spatial resolution of our set-up does not seriously distort the correct hydrodynamic velocity patterns over scales large as compared to the cellsize.

$y(t) > 0$,] of the atmosphere shows expanding patches or ‘clusters’ ($v_z(t; x, z) > 0$) [contracting patches: $v_z(t; x, z) < 0$] of various sizes in a contracting [expanding] ‘sea’ (Fig. 1); the area occupied by these clusters then grows until the individual clusters join, in a manner reminiscent of a percolation phase transition. The microstates of the motion thus exhibit a succession of such percolation phase transitions; clusters of expansion [contraction] grow and become more numerous until they merge into one or several large clusters; then the same process is repeated all over again. It is the alternation of a dominance of expanding areas with a dominance of contracting areas that creates the illusion of the overall regularity, encoded in the cyclic temporal pattern of $y(t)$: Globally, the velocity field appears to pulsate radially with a small amplitude, while locally it exhibits spatio-temporal variability. The macrostate variable $y(t)$ traces this average cyclic variation, of amplitude nearly an order of magnitude less than the amplitude of the local velocity.⁶

It transpires that this intricate spatio-temporal velocity pattern must obey an irreducibly complex dynamics. It seems also quite clear that the actual atmosphere behaviour generated in the CA experiment exhibits what is referred to in the literature as Large-Scale Chaos, a strong variant of chaos requiring a dynamics defined in an irreducible high-dimensional phase space.

Fig. 2 illustrates the time series $y(t)$ over 3000 CA timesteps, every tenth step being shown; plotted steps are listed as $t = 1, 2, \dots, 300$ (t expressed in 10 CA timesteps). The noisy macrostate observable $y(t)$, although generated from an underlying complex kinematics $\mathbf{v}(t; \mathbf{r})$, has a well-defined cycle length fluctuating around an average of 215 CA timesteps (order of twice the sound propagation time from bottom to top of the atmosphere). The average y -amplitude is of the order of 0.03 in CA units, while the local radial velocity $v_z(t; x, z)$ exceeds 0.2 in CA units; the plotting scale, 0 to 120 of Fig. 2 corresponds to a velocity range -0.06 to $+0.06$ CA units.

3. Neural network analysis and filtering

We have insisted on the high amount of noise generated in our LG procedure which implies in turn that the time series $y(t)$ itself remains noisy: The latter exhibits large irregular fluctuations around an underlying systematic time pattern (Fig. 2). The physical origin of these residual fluctuations can be described as follows. The clusters of local expansion or contraction obey a time-dependent statistical distribution. The ideal macropulsation variable, $s(t)$, should then represent the average with respect to this distribution, namely a smooth cyclic pattern from which all statistical fluctuations (small size and number effects) are erased. The physical origin of the residual fluctuations is made more transparent if instead of $y(t)$ we consider an al-

⁶ The existence of a stationary large amplitude activity on small spatial scales is best demonstrated by an animation of the sequence of flow patterns (cf. Lejeune and Perdang 1993). Thereby the variability of the pulsation microstructure is clearly exhibited (creation, growth, dissolution of short-lived localised large-amplitude velocity patterns). The low-amplitude macropulsational effect is harder to notice in the animation.

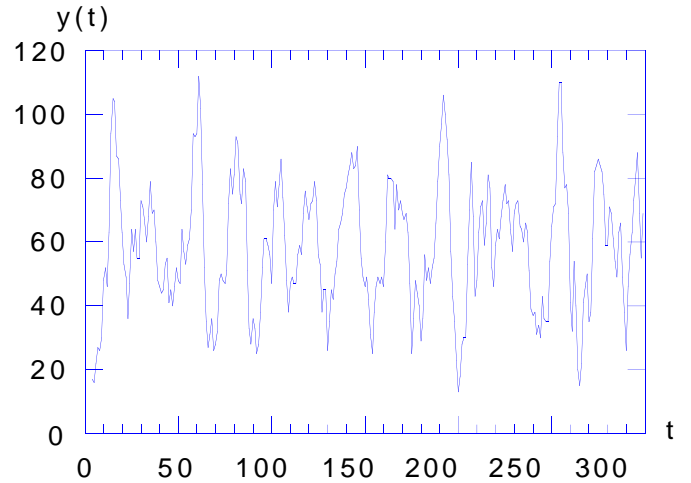


Fig. 2. Time series $y(t)$ of the LG atmosphere model in the stationary phase (unit of time = 10 CA timesteps; scale 0 to 120 corresponds to -0.06 to $+0.06$ CA velocity units).

ternative series $y'(t) = 2[A_+(t)/A] - 1$, where $A_+(t)$ and A represent the observable area of the clusters of local expansion at a given epoch t and the total observable area of the star respectively (note the analogy with a sunspot number); this series carries essentially the same information as $y(t)$. The underlying regularity of $y'(t)$ is here the result of the average statistics of the expanding patches; individual expanding patches are created, while others are destroyed, and individual patches are growing while others at the same time are shrinking; accordingly the global area $A_+(t)$ changes rather smoothly and slowly due to the compensations of creations and destructions, and of shrinkings and growings of the clusters; if strong fluctuations in the time pattern $y'(t)$ still survive, then this is a consequence of the small number of patches, or equivalently, of the small total area A ; these fluctuations would be suppressed in $y'(t)$ if we could work out the analogue of a thermodynamic limit, $A \rightarrow \infty$. The purpose of this section is to obtain an acceptable approximation to the underlying smooth cyclic pattern, $s(t)$, without constructing this limit. To this end we apply a signal-adapted filtering operation capable of eliminating high amplitude fluctuations, provided that these fluctuations occur on a timescale short with respect to the cycles.

It has been stressed that Neural Networks (NNs) are formally nonlinear versions of the standard Wiener filter (cf. Lahav 1994). An adequately designed NN should therefore be able to operate as an efficient noise filter. When set up as an adaptive dynamical system of given (low) dimension d , an NN theoretically achieves a strong filtering of intrinsically d -dimensional signals, by construction. Numerical experiments have confirmed for instance that from a noise-corrupted signal generated by the logistic map the original noise-free signal is recovered by an NN analysis of the noisy signal (Albano et al 1992; cf. also the NN treatment of meteorological time series by Murtagh and coworkers; Aussem et al 1994, 1995). However, as pointed out elsewhere (Perdang 1997), the currently standard set-up of an NN in the form of a d -dimensional dynamical system is rigorously justified as a

filtering device only if we know a priori that the signal has been generated by a dynamical system of dimension $\leq d$ (as was the case in the test experiment of Albano et al 1992). In the case of observational stellar time series, this requirement is not satisfied (cf. our Introduction).

On the other hand, the 3-layer perceptron scheme discussed in Perdang (1997) is an NN capable of simulating signals generated by a dynamics of *arbitrary* dimension. Moreover, if a carefully selected auxiliary signal-adapted reference function, $W(t; V^1(t), \dots, V^m(t))$, is adopted to reconstruct the observed time series, then experience shows that a smooth signal is extracted from the raw data, even in the presence of large-amplitude noise. The reference function is regarded as an m parameter function $W(t; V^1, \dots, V^m)$, chosen such that we can find constants, V_o^1, \dots, V_o^m , for which the presumed main features of the noise-free signal $s(t)$ are reproduced by $W(t; V_o^1, \dots, V_o^m)$; in the proper NN analysis these constants V_o^1, \dots, V_o^m then become adjustable *functions* of the epoch t , to be synthesised on the NN. The use of the signal-adapted reference function thus allows us to control the nature of the time pattern we want to reproduce. In addition it can speed up the learning process of the NN considerably.

For the specific task of noise suppression we adopt a perceptron of architecture $P[N_1\{2\}; N_2\{2\}; N_3\{z_3\}]$, with N_1 , N_2 , and N_3 , nodes in the input layer, in the hidden layer, (coded in binary form) and in the the output layer (in base z_3) respectively. Given the signal $y(t)$, $t = 0, 1, \dots, T - 1$, the epoch t is carried by the input layer; the number of nodes N_1 is thus fixed by the length T of the time interval, and the binary base of the coding. The (minimal) number of nodes of the hidden layer, N_2 , required to achieve the learning precision, is automatically adjusted in the program. Finally, the number of nodes in the output layer, N_3 , is set equal to the number m of dependent variables in the trial function W ; the latter nodes are coded in a high enough base z_3 determined by the resolution of the signal (cf. Perdang 1997 for the technical details).

In our case, the choice of the signal-adapted trial function is guided by the following considerations. The time series shows a seemingly monocyclic behaviour (cf. Fig. 2); our first goal is then to identify these cycles. The amplitudes of the observed cycles are deformed by large fluctuations (cf. our physical interpretation); a second goal is then to generate a smooth pattern by suppressing the short-time fluctuating component. The simplest reference function achieving a smooth monocyclic behaviour is a sine wave; therefore we choose the reference function in the form

$$W(t; A(t), P(t)) \equiv A(t) \cos(2\pi \frac{t}{P(t)} + \phi). \quad (3.1)$$

This representation involves 2 free functions, namely an epoch-dependent amplitude, $A(t)$, and an epoch-dependent period $P(t)$; without loss the phase ϕ is kept constant. The phase ϕ , together with the constant reference amplitude and period, A_o and P_o , are chosen such as to give an optimal fit of the reference trial signal $W(t; A_o, P_o)$ to the observed signal $y(t)$. For a noise level ν (to be defined), the free functions $A(t)$ and $P(t)$

are to be adjusted by the perceptron so as to satisfy the condition $\|W(t; A(t), P(t)) - y(t)\| < \nu$, (with the norm to be defined); thereby the perceptron tries to keep functions $A(t)$, $P(t)$ close enough to the reference constants A_o and P_o . It is through this latter effect that the selected trial signal guides the reconstruction of the noise-free signal $s(t)$.

Denote by q the collection of ‘learning’ parameters of the NN (synaptic weights, etc; cf. Perdang 1997). For a given set of parameter values q , the perceptron, when ‘stimulated’ on the input layer by an integer t ($= 0, 1, \dots, \text{or } T - 1$), generates a ‘response’ $A(t; q), P(t; q)$ on the two output nodes which depends on the values q . The perceptron reconstruction of the signal, $y_P(t; q)$, is then achieved through representation (3.1), $y_P(t; q) \equiv W(t; A(t; q), P(t; q))$. The process of ‘learning’ consists in seeking an eventual collection of parameter values q_{fin} such that the final perceptron signal $y_P(t; q_{\text{fin}})$ reproduces the original signal $y(t)$ within the noise level. This reconstruction, $s(t)$, is a noise-free version of the original signal $y(t)$.

The NN parameters are initially set equal to reference values q_o such that $A(t; q_o) \equiv A_o, P(t; q_o) \equiv P_o$, so that the trial signal $W(t; A_o, P_o)$ is reproduced *exactly* on the perceptron. It is indeed always possible to determine analytically reference values $q = q_o$ (and more generally, ranges of values), such that the node states of the output layer are independent of the node states of the input layer (cf. Perdang 1997). Thus

$$y_P(t; q_o) \equiv W(t; A_o, P_o). \quad (3.2)$$

Consider then the auxiliary homotopic family

$$y_\lambda(t) = (1 - \lambda) W(t; A_o, P_o) + \lambda y(t), \quad 0 \leq \lambda \leq 1. \quad (3.3)$$

The function $y_\lambda(t)$ continuously deforms the reference trial signal, $y_o(t) \equiv W(t; A_o, P_o)$, into the actual signal to be analysed, $y_1(t) \equiv y(t)$, as the parameter λ increases from 0 to 1. The *learning* of the NN then consists in progressively incrementing λ in Eq. 3.3 from 0 (NN parameters $q = q_o$ exactly known) to 1 (final NN parameters $q = q_{\text{fin}}$ achieving the ‘best’ auxiliary functions $A(t), P(t)$ in representation 3.1) by applying a *Diffusion Algorithm* at each step in λ (Perdang 1997, 1998): Essentially, q executes a random walk in the parameter space around its ‘best’ position at the previous λ level, until the perceptron signal $y_P(t; q)$ approximates $y_\lambda(t)$ with the precision fixed by the noise level ν . The procedure is ended at $\lambda = 1$, when q has diffused to a point q_{fin} such that the discrepancy between

$$s(t) \equiv y_P(t; q_{\text{fin}}), \quad (3.4)$$

and the original signal $y(t)$ is less than the precision (ν). In our numerical experiments we measure precision by the relative Euclidean distance between the original time series $y(t)$ and the perceptron signal $y_P(t; q)$; the noise level, i.e. the level of the fluctuations we want to get rid of, has been estimated as $\nu \approx 10\%$.

The final NN signal reproduction, $s(t)$, obtained by this method is shown in Fig. 3 (continuous curve), together with the original signal $y(t)$ (dotted curve). As a test calculation we carried out the learning process for the time series $y(t)$ from

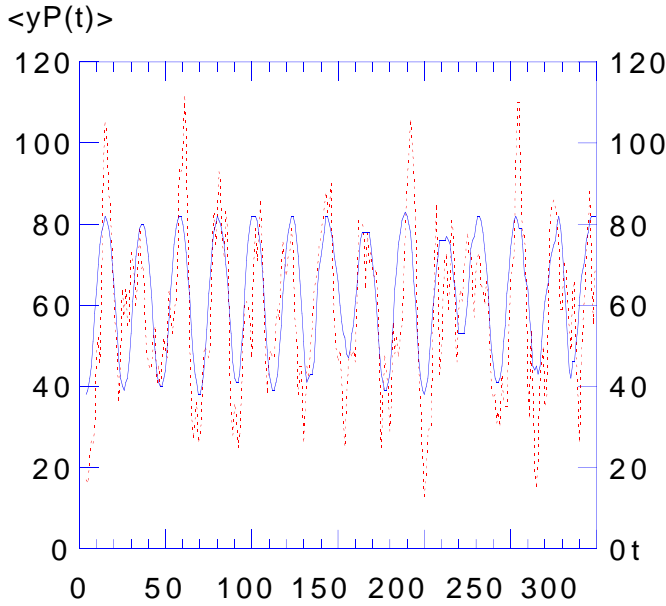


Fig. 3. The original signal $y(t)$ (dotted) and the NN-filtered signal $s(t)$ (continuous).

which 20% of the data points were missing, namely 30 adjacent points of the middle of the range (2 peaks), together with the last 30 points (2 peaks). The learning parameters q_{fin} were then adjusted with a precision of 11.5%. With the values q_{fin} the perceptron predicts the missing stretches of the series with a precision of 9.9%; the precision of the extrapolation and interpolation is thus of the same order as the learning precision. The fact that prediction—over a limited range—is possible is indicative that the noisy time series $y(t)$ does indeed contain a systematic deterministic component.

The NN-filtering operation is seen to have the following effect on the original series $y(t)$.

- (a) It smoothes out the short-time structure in the original cycles (cf. the cycle near $t = 20$).
- (b) It levels off the highest maxima (near epochs $t = 15, 60, 190$ and 255) and lowest minima (near $t = 5, 200$ and 265).
- (c) It uncovers cycles hidden within the noise (the 2 cycles in the range $200 < t < 240$).

The final filtered signal $s(t)$ (Fig. 3) looks surprisingly regular. It can be seen, however, that the individual cycles are not identical. The local amplitude $A(t)$ and period $P(t)$ as synthesised on the perceptron vary with the epoch. This behaviour is clearly exhibited by a plot of the phase space trajectory in a trial 3D space, of coordinates $X = s(t)$, the filtered signal itself (a formal radial *velocity*), $Y = \int dt s(t) = \Delta R(t)$ (a formal *radius variation*), and $Z = d/dt s(t) = a(t)$ (a formal radial *acceleration*) (Fig. 4). The advantage of this choice of trial phase space coordinates over the conventional delayed coordinates is the avoidance of an extra parameter of time delay (cf. Perdang 1993). The stereoscopic representation of Fig. 4 shows a cloud of points concentrated in a toroidal zone of the 3D space.



Fig. 4. Stereoscopic view of the 3D trial phase space trajectory associated with the filtered signal $s(t)$ (origin of coordinate system at centre of each cloud; axes X: horizontal; Y: vertical; Z: towards observer).

4. Reconstruction of signal dynamics

The discussion of the physical interpretation of the ideal macropulsation signal outlined in the previous section legitimates our belief that the NN-filtered signal (Eq. 3.4) is an optimal representation of the latter. Knowing this representation, we can then directly address the question of estimating the minimal dimension d_* of the ideal signal dynamics Δ_* . From an inspection of the 3D trial phase space (Fig. 4) it is obvious at the outset that we have the constraint $d_* \geq 3$.

To reconstruct the dynamics Δ_* from the signal $s(t)$ (Eq. 3.4) we apply the method devised by Serre et al (1996, 1996a). In principle this approach amounts to finding the lowest order ODE in the form

$$d/dt S = v(S), \tag{4.1}$$

where $S(t)$ is the delay vector associated with the signal $s(t)$

$$\begin{aligned} S(t) &= (s_1(t), s_2(t), \dots, s_{d'}(t)) \\ &\equiv (s(t), s(t + \tau), s(t + 2\tau), \dots, s(t + (d' - 1)\tau)). \end{aligned} \tag{4.2}$$

As usual τ denotes the delay, treated as a free parameter; $v(S)$ is the phase space ‘velocity vector’, of trial dimension d' , to be estimated in the method. In the actual computational procedure the ODE (4.1) is approximated by an iteration

$$S(t + 1) = F(S(t)), \tag{4.3}$$

the map $F(S(t))$ being the function to be estimated from the time series $s(t)$. The approach then consists in expanding the map $F(S)$ in a truncated series of orthogonal polynomials; the expansion coefficients c play the parts of adjustable parameters (cf. Serre et al 1996 for the technicalities of the method). For a given delay τ and a given trial dimension d' , ‘best’ coefficients $c = c(d', \tau)$ are derived from the actual time series $s(t)$; this specifies a trial dynamical system (4.3). Solving the latter for

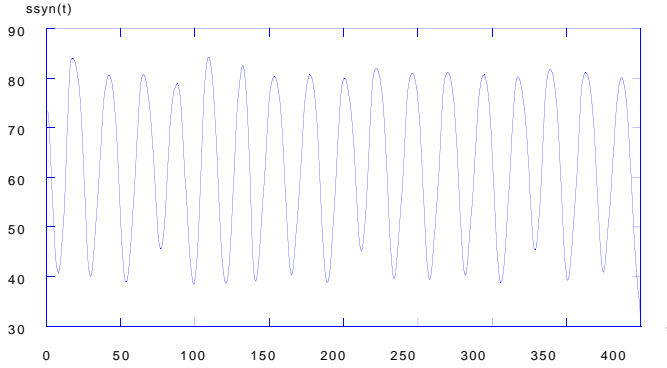


Fig. 5. An example of a synthetic signal $s_s(t)$ obtained from an integration of the 4D signal dynamics.

initial conditions close to the attractor carrying the series $s(t)$, we generate synthetic trial series, $s(t; d', \tau, c(d', \tau))$. The main characteristics (power spectrum, phase space behaviour, Lyapunov exponents) of these trial signals are compared with those of the actual signal $s(t)$. Given a precision factor ϵ , if

$$\| s(t) - s(t; d', \tau, c(d', \tau)) \| \leq \epsilon \quad (4.4)$$

for a Euclidean norm chosen over some timestretch (\leq the Lyapunov horizon in the case of chaos), then the trial dynamics is an acceptable signal dynamics (to the precision ϵ), provided that the main characteristics of the solutions are compatible with those of the actual signal $s(t)$. The lowest dimension d_* consistent with these conditions under variations of τ , and variations of the maximum degree of the polynomial expansions, then specifies the reconstructed signal dynamics Δ_* .

The application of this method to our filtered signal $s(t)$ (Fig. 3) yields a minimum phase space dimension $d_* = 4$. An instance of a synthetic signal

$$s_s(t) \equiv s(t; d_*, \tau_*, c(d_*, \tau_*)) \quad (4.5)$$

solution of Eq. (4.3) is exhibited in Fig. 5.

A closer analysis of the synthetic time series generated from the reconstructed signal dynamics indicates in fact that these series possess the typical features of the original signal $s(t)$. The specific signal of Fig. 5 is characterised by one unstable Lyapunov exponent, $\lambda_+ = 1.72 \cdot 10^{-2}$ in the time units of Figs. 2, 3 and 5 (10 CA timesteps), one zero exponent (numerical estimate : $\approx 4.5 \cdot 10^{-3}$), and two negative exponents (-0.019 and -0.102); the corresponding Lyapunov dimension of the attractor is 3.03. Although close to 3, this value cannot be interpreted as the dimension of a 3-torus (attractor of a triple-periodic regular oscillation); the existence of one positive Lyapunov exponent clearly indicates that the signal is chaotic. A precise duplication by a synthetic signal of the original series $s(t)$, over the full interval of observation, is not to be expected. The Lyapunov timescale, $T_L = 1/\lambda_+ \approx 58$, is indeed about 3 cycle lengths. Accordingly, prediction over 3 cycles remains reasonably accurate, as we have already noticed experimentally (cf. Sect. 3). But over times $\gg T_L$ the chaotic nature of the signal dynamics renders precise prediction impossible. A closer numerical

exploration of the 4D signal dynamics (4.3) indicates that the phase space trajectories remain bounded, and seemingly trapped in a toroidal region, for any initial condition close to the original signal $s(t)$.

We conclude that the reconstructed signal dynamics Δ_* possesses a strange attractor of Lyapunov dimension close to 3.

The main results of this section, namely (a) the existence of a signal dynamics of *low dimension* ($d_* = 4$), and (b) the presence of *chaos* in the synthetic signals, are not surprising in the light of the general comments made in the Introduction. The local complexity of the actual velocity field of our simulated stellar atmosphere (cf. Fig. 1) definitely excludes a low dimensional model dynamics Δ responsible for the micropulsations; but the latter dynamics contains an *approximate* closed subdynamics Δ_* formally obtained (a) by collapsing large numbers of microscopic degrees of freedom into collective macroscopic degrees of freedom (dimensional reduction); and (b) by ignoring couplings with the microscopic details of the motion, on the level of precision ν (closure). This reduction is essentially similar to the reduction of an N-body dynamics to a low order fluid dynamics scheme.

The origin of chaos in the subdynamics Δ_* can be due to two causes. On the one hand the chaotic behaviour of the reduced system may be *intrinsic*, the chaos being reproducible by a simple physical model described by the equations of Δ_* . Alternatively, there is a more subtle possibility for generating chaos. If the perturbations of the micropulsations on the full dynamics Δ have a cumulative effect on the macropulsational signal $s(t)$ (cf. Introduction), then prediction from the subdynamics Δ_* cannot remain reliable beyond a certain time T_* , since the latter is not an exact autonomous subdynamics of the full dynamics Δ . Failure of predictability can then be forced into the reconstructed dynamics Δ_* by creating an *extrinsic* artificial chaos of Lyapunov horizon $\approx T_*$: In low-dimensional dynamical systems of format (4.3), this deterministic chaos is in fact the only type of behaviour consistent with a lack of predictability.

5. Discussion and conclusion

In our 2D CA simulations of stellar pulsations the experimental time series $y(t)$ (Eq. 2.2), and the filtered version thereof, $s(t)$ (Eq. 3.4), mimic a radial velocity, while the actual velocity field of the model atmosphere has an involved 2D spatio-temporal structure (termed the pulsational microstates in this paper). The dynamics accounting for the micropulsations is not low-dimensional. Our experiments indicate that the strong noisy component in our observable $y(t)$, which appears as superimposed on a fairly regular pattern (Fig. 2), is the result of the local details of the fluid motions (micropulsations). Ideally, and in principle, this physical noise could be eliminated if we could go to the limit of an atmosphere of infinite extension. A major problem we addressed in this work consisted in devising a procedure capable of sifting out this physical noise and of extracting the smooth underlying systematic component without going through the artificial limit process; the limit process is not applicable to realistic spherical stellar models anyway. The

approach which proves useful and efficient consists in carrying out an NN filtering of the signal, based on a signal-adapted trial function which possesses the main qualitative features of the signal we wish to recover (Sect. 3). The final smooth signal $s(t)$ we obtain in this way is found to be reproducible by a low-dimensional dynamics ($= 4$, Sect. 4), similar to the dynamics of purely radial pulsations.

We then have here an instantiation of alternative (2) listed in the Introduction. The signal dynamics Δ_* as derived from the empirical time series $y(t)$ (the observer's radial velocity curve $v(t)$) is of low dimension. Traditionally such a result is simply interpreted by saying that the stellar hydrodynamics is equivalent with a dynamical system of low dimension (a low-order ODE), and, possibly, that the pulsation is purely radial. Our experiments deny such a conclusion; the detailed hydrodynamic velocity field (Fig. 1) requires a fundamental dynamics Δ of very high complexity.

On a more general and more abstract basis, our experiments show that a dynamical system Δ of high dimension d (possibly exhibiting Large-Scale Chaos) may well possess a collection of d_* independent observables $R(t)$ attached with it which obey a closed autonomous (generally approximate) subdynamics Δ_* of low dimension $d_* \ll d$. Formally, the existence of such observables can be viewed as extensions of conservation laws or approximate conservation laws associated with the dynamics Δ : Instead of obeying $d/dt R = 0$, as is the case for standard conservation laws, we have here a d_* -dimensional system $d/dt R = G(R)$; each component of R is a function of the variables of the dynamics Δ . For conventional conservation laws the functions $R = \text{constant}$ constrain the allowed solutions of the full dynamics Δ to evolve on manifolds or on more general geometrical sets in the d -dimensional phase space. In contrast, with the geometrical sets associated with ordinary conservation laws, the sets defined by the time-dependent functions, $R = \rho(t)$, become time-dependent themselves. The representative point of the dynamics Δ is thus carried by a time-dependent support in the d -dimensional phase space.

In the case of the observed stellar radial velocity curve, $v(t)$, the associated signal dynamics Δ_* is not explicitly known theoretically, say in the form of an ODE (1.5) analytically derived from the stellar fluid dynamics Δ . Our experiments indicate, however, that the signal $y(t)$ (and $v(t)$) possesses the characteristic features of the velocity curve of a true radial pulsation. It then seems perfectly reasonable to attempt to describe the behaviour of the latter by a fictitious *radial* hydrodynamics, namely by formal equations of same format as the standard radial hydrodynamics. The difference with the latter consists in that the constitutive equations we have to deal with must include contributions due to the micropulsation states. In other words, the conventional (particle and radiation) pressure, P , the internal energy, U , etc, must be replaced with a pressure P_* , an internal energy U_* , etc, including the effects of the various averages involving the deviations of the micropulsations from the macropulsations. Attempts at devising such kinetic and thermodynamic descriptions of the specific contributions of turbulent

motions were sought for in the past; but no physically viable closed scheme has emerged so far.

The result of our numerical experiments may be construed as an argument in favour of the *existence* of such a fictitious radial dynamical description. Since the signal dynamics Δ_* is then equivalent to the proposed fictitious radial dynamics, in principle, the unknown constitutive equations, or at least strong constraints on the latter, can then be derived empirically, from the reconstructed signal dynamics.

Finally, what our experiments really suggest is that a fully satisfying context for analysing stellar pulsations is a detailed theory of nonlinear nonradial pulsations. Only within that general framework, solved for generic initial conditions, can we be reasonably sure that we do not miss out observationally relevant pulsation patterns.

Acknowledgements. This work was supported in part by two Royal Society-FNRS European Exchange Grants (JP 1996, 1997). The authors wish to thank the referee, M.J. Goupil, for her careful reading of the manuscript.

References

- Albano A.M., Passamante A., Hediger T., Farrell M.E., 1992, *Physica* D58, 1
- Aussem A., Murtagh F., Sarazin M., 1994, *Vistas in Astronomy* 38, 375
- Aussem A., Murtagh F., Sarazin M., 1995, 'Dynamical Recurrent Neural Networks - Towards Environmental Time Series Prediction' (preprint)
- Benz W., Herant M., 1993, in : *Cellular Automata: Prospects in Astrophysical Applications*, World Scientific, Singapore, p. 369
- Buchler J.R., Kollath Z., Serre T., Mattei J., 1996, *The Astrophysical Journal* 462, 489
- Casdagli M., 1989, *Physica* D35, 335
- Farmer J.D., Sidorovich J.J., 1987, *Physical Review Lett.* 59, 845
- Farmer J.D., Sidorovich J.J., 1988, in : *Evolution, Learning and Cognition*, edit.: Lee Y.C., World Scientific, Singapore
- Fryxell B., Arnett D., Müller E., 1991, *The Astrophysical Journal* 395, 642
- Gershenfeld N.A., Weigend A.S., 1993, in : *Time Series Prediction : Forecasting the Future and Understanding the Past*, edits.: Weigend A.S., Gershenfeld N.A., Addison Wesley, p. 1-70
- Goupil M.J., Auvergne M., Baglin A., 1988, *Astronomy and Astrophysics Letters* 196, L13
- Hachisu I., Matsuda T., Shigezuma T., Nomoto K., 1990, *The Astrophysical Journal Lett.* 358, L57
- Lahav O., 1994, *Vistas in Astronomy* 38, 251
- Lejeune A., Perchang J. (editors), 1993, *A Video on CA Models in Astrophysics* (sequence 5), LEM, Liège, and Médiathèque de Strasbourg
- Lejeune A., Perchang J., Raty J.Y., 1994, in : *Proceedings of the 6th Joint EPS-ASP International Conference on Physics Computing*, edits: Gruber R., Tomassini M., European Physical Society, Geneva, p. 527
- Perchang J., 1990, in : *Cours de Structure Interne, Aussois, 2e Session*, edits.: Hubert A.M., Schatzman E., Observatoire de Paris, pp. 311-456
- Perchang J., 1991, in : *Rapid Variability of OB-Stars: Nature and Diagnostic Value*, ESO Conference and Workshop Proceedings 36, 349

- Perdang J., 1993, in : Cellular Automata: Prospects in Astrophysical Applications, World Scientific, Singapore, p. 341
- Perdang J., 1994, Astrophysics and Space Science 220, 1
- Perdang J., 1997, Annals of the New York Academy of Sciences 808,214
- Perdang J., 1998, 'Neural Network Assisted Analysis of the Lightcurves of Cataclysmic Variables' (in preparation)
- Serre Th., 1992, PhD Thesis, Observatoire de Paris (unpublished)
- Serre Th., Buchler J.R., Goupil M.J., 1991, in: White Dwarfs, edits.: Vauclair G., Sion E., Kluwer, The Netherlands, p. 175
- Serre Th., Kollath Z., Buchler J.R., 1996, Astronomy and Astrophysics 311,833
- Serre Th., Kollath Z., Buchler J.R., 1996a, Astronomy and Astrophysics 311, 845